



Inactivation of Cerebral Cavernous Malformation Genes Results in Accumulation of von Willebrand Factor and Redistribution of Weibel-Palade Bodies in Endothelial Cells

OPEN ACCESS

Edited by:

Sanyuan Ma,
Southwest University, China

Reviewed by:

Ruben Bierings,
Erasmus Medical Center, Netherlands
Andreas Fischer,
German Cancer Research Center
(DKFZ), Germany

***Correspondence:**

Stefanie Spiegler
spiegler@uni-greifswald.de

[†]Present address:

Center for Innovation Competence
(ZIK) - Humoral Immune Reactions in
Cardiovascular Diseases, University of
Greifswald, Greifswald, Germany

Specialty section:

This article was submitted to
Molecular Diagnostics and
Therapeutics,
a section of the journal
Frontiers in Molecular Biosciences

Received: 28 October 2020

Accepted: 21 June 2021

Published: 09 July 2021

Citation:

Much CD, Sendtner BS, Schwefel K,
Freund E, Bekeschus S, Otto O,
Pagenstecher A, Felbor U, Rath M and
Spiegler S (2021) Inactivation of
Cerebral Cavernous Malformation
Genes Results in Accumulation of von
Willebrand Factor and Redistribution of
Weibel-Palade Bodies in
Endothelial Cells.
Front. Mol. Biosci. 8:622547.
doi: 10.3389/fmolb.2021.622547

Christiane D. Much¹, Barbara S. Sendtner¹, Konrad Schwefel¹, Eric Freund²,
Sander Bekeschus², Oliver Otto³, Axel Pagenstecher⁴, Ute Felbor¹, Matthias Rath¹ and
Stefanie Spiegler^{1*†}

¹Department of Human Genetics, Interfaculty Institute of Genetics and Functional Genomics, University Medicine Greifswald, Greifswald, Germany, ²Centre for Innovation Competence (ZIK) plasmatis, Leibniz Institute for Plasma Science and Technology (INP), Greifswald, Germany, ³Centre for Innovation Competence (ZIK) - Humoral Immune Reactions in Cardiovascular Diseases, University of Greifswald, Greifswald, Germany, ⁴Department of Neuropathology, Center for Mind, Brain and Behavior (CMBB), University Hospital Giessen and MarburgMarburg, Germany

Cerebral cavernous malformations are slow-flow thrombi-containing vessels induced by two-step inactivation of the *CCM1*, *CCM2* or *CCM3* gene within endothelial cells. They predispose to intracerebral bleedings and focal neurological deficits. Our understanding of the cellular and molecular mechanisms that trigger endothelial dysfunction in cavernous malformations is still incomplete. To model both, hereditary and sporadic CCM disease, blood outgrowth endothelial cells (BOECs) with a heterozygous *CCM1* germline mutation and immortalized wild-type human umbilical vein endothelial cells were subjected to CRISPR/Cas9-mediated *CCM1* gene disruption. *CCM1*^{-/-} BOECs demonstrated alterations in cell morphology, actin cytoskeleton dynamics, tube formation, and expression of the transcription factors KLF2 and KLF4. Furthermore, high VWF immunoreactivity was observed in *CCM1*^{-/-} BOECs, in immortalized umbilical vein endothelial cells upon CRISPR/Cas9-induced inactivation of either *CCM1*, *CCM2* or *CCM3* as well as in CCM tissue samples of familial cases. Observer-independent high-content imaging revealed a striking reduction of perinuclear Weibel-Palade bodies in unstimulated *CCM1*^{-/-} BOECs which was observed in *CCM1*^{+/-} BOECs only after stimulation with PMA or histamine. Our results demonstrate that CRISPR/Cas9 genome editing is a powerful tool to model different aspects of CCM disease *in vitro* and that *CCM1* inactivation induces high-level expression of VWF and redistribution of Weibel-Palade bodies within endothelial cells.

Keywords: cerebral cavernous malformation, *CCM1*, blood outgrowth endothelial cells, CRISPR/Cas9, von Willebrand factor

INTRODUCTION

Cerebral cavernous malformations (CCMs) are convolutes of dilated capillaries in the central nervous system. Familial occurrence of multiple CCMs (OMIM 116860, 603284, 603285) is associated with autosomal-dominantly inherited loss-of-function variants in one of the three genes *CCM1* (*KRIT1*, OMIM: *604214), *CCM2* (Malcavernin, *OSM*, *607929) or *CCM3* (*PDCD10*, *TFAR15*, *609118). In agreement with a Knudsonian two-hit mechanism, somatic inactivation of the corresponding wild-type allele in vascular endothelial cells (ECs) is widely accepted as the critical step in CCM initiation (Gault et al., 2005; Akers et al., 2009; Pagenstecher et al., 2009; McDonald et al., 2014; Rath et al., 2020). In patients without a pathogenic germline variant, two biallelic somatic mutations are thought to cause CCM disease (McDonald et al., 2014).

Since the first reports of disease-causing *CCM1* variants in familial CCM cases (Laberge-le Couteulx et al., 1999; Sahoo et al., 1999), we have learned a lot about CCM pathogenesis and the endothelial dysfunction in cavernous lesions (Maddaluno et al., 2013; Cuttano et al., 2016; Zhou et al., 2016; Detter et al., 2018; Malinverno et al., 2019; Hong et al., 2020; Ren et al., 2021). A first expert consensus guideline and clinical recommendations for CCM management have been published in recent years (Akers et al., 2017; Flemming and Lanzino, 2020). However, there are still no effective drugs that would prevent cavernoma formation or CCM bleeding. A recent prospective population-based study revealed that antithrombotic therapy – anticoagulant as well as antiplatelet – is associated with a lower risk of intracranial hemorrhage and focal neurological deficits (Zuurbier et al., 2019). These counterintuitive data are consistent with a neuropathological study that anticipated a dysfunction of cavernous ECs which would result in local organizing thrombi as the primary step causing repeated secondary microhemorrhages and disease progression (Abe et al., 2005). The multimeric von Willebrand factor (VWF) protein is an important player in primary hemostasis. VWF is almost exclusively expressed by vascular ECs and bone marrow megakaryocytes (Lip and Blann, 1997). In the vascular endothelium, VWF is stored in Weibel-Palade bodies (WPBs) which secrete their prothrombotic content through exocytosis (Weibel and Palade, 1964; Sadler, 1998; Wagner and Frenette, 2008). Secretion of large amounts of VWF from WPBs can be triggered by shear stress or stimulation with Ca^{2+} raising agents like histamine, thrombin or vascular endothelial growth factor (VEGF) (Loesberg et al., 1983; Erent et al., 2007).

Using CRISPR/Cas9-based *in vitro* modeling of hereditary and sporadic CCM disease, we here demonstrate that the inactivation of *CCM1*, *CCM2* or *CCM3* in ECs induces intracellular VWF accumulation and WPB redistribution. Analyses of human CCM tissue samples support the hypothesis that increased VWF levels in the endothelium of distended caverns contribute to the local hemostatic imbalance in these fragile vascular lesions.

MATERIALS AND METHODS

Cell Culture

The generation of blood outgrowth endothelial cells (BOECs) from a CCM proband with a pathogenic *CCM1* germline variant (*CCM1*^{+/-}) has been described before (Spiegler et al., 2019). Immortalized human umbilical vein endothelial cells (CI-huVECs) were obtained from InSCREENex (Braunschweig, Germany) and maintained in complete endothelial cell growth medium (ECGM; PromoCell, Heidelberg, Germany) supplemented with 10% fetal calf serum (FCS; Thermo Fisher Scientific, Waltham, MA, United States). Tube formation was performed in 384-well microplates. In brief, 17 μ l Matrigel (Corning, Kaiserslautern, Germany) was incubated at 37 °C for 1 h. Next, 8,000 cells were seeded. After 16 h, tube formation was imaged and quantified with the angiogenesis analyzer for ImageJ (<https://imagej.net>). To stimulate secretion of WPBs, cells were grown on 96- or 6-well plates, preincubated with Opti-MEM (Thermo Fisher Scientific) for 1 h and treated solely in Opti-MEM or with dimethyl sulfoxide (DMSO, Carl Roth, Karlsruhe, Germany), 150 nM Phorbol 12-myristate 13-acetate (PMA, Cayman Chemical, Ann Arbor, MI, United States), 100 μ M Histamine (Sigma-Aldrich, St. Louis, MO, United States), 1 μ M Desmopressin (Acetate) (DDAVP, MedChem Express, Sollentuna, Sweden) or 1 μ M DDAVP plus 100 μ M 3-Isobutyl-1-methylxanthine (IBMX, Sigma-Aldrich, St. Louis, MO, United States) in Opti-MEM for 1 h according to Wang and colleagues (Wang et al., 2013).

CRISPR/Cas9-Mediated Gene Editing

CCM1^{-/-} BOECs were generated with CRISPR/Cas9 genome editing from *CCM1*^{+/-} BOECs as described before (Spiegler et al., 2019). In brief, *CCM1*^{+/-} BOECs were transfected with crRNA:tracrRNA:Cas9 ribonucleoprotein (RNP) complexes that were specific to the *CCM1* wild-type allele. Upon confluence on T25 flasks, the CRISPR/Cas9-treated cell mixture was seeded on 96-well plates with an average cell density of 0.5 cells/well. Emerging BOEC clones were genotyped by next generation sequencing in a custom two-step PCR enrichment approach. PCR products were pooled after purification with Agencourt AMPure XP beads (Beckman Coulter, Brea, CA, United States) and sequenced with 2 × 150 cycles on a MiSeq instrument (Illumina, San Diego, California, United States of America). The SeqNext software was used for data analysis (JSI Medical Systems, Eettenheim, Germany). Only variants with quality scores ≥ 30 were called. BOEC clones with biallelic *CCM1* loss-of-function variants (*CCM1*^{-/-}) were selected for further expansion. Three to four individual *CCM1*^{+/-} BOEC lines that had been clonally expanded from the blood of the CCM proband were used as controls. For complete knockout of *CCM1*, *CCM2* and *CCM3* in CI-huVECs, the following Alt-R CRISPR-Cas9 crRNAs (Integrated DNA Technologies (IDT), Coralville, Iowa, United States of America) were used: 5'-GGAGCTCCTAGACCAAAGTA-3' (*CCM1*), 5'-GGTCAGTTAACGTCCATACC-3' (*CCM2*), and 5'-CAACTCACCTCATTAACAC-3' (*CCM3*). A non-targeting crRNA (nc crRNA #1, IDT) served as control. Reverse transfection, estimation of the genome editing

efficiencies by T7 endonuclease I digestion or Sanger sequencing, and the expansion of knockout CI-huVEC clones were performed as delineated previously (Schwefel et al., 2019; Spiegler et al., 2019; Schwefel et al., 2020).

Immunofluorescence Analyses

After fixation of the cells on 96-well plates with 4% paraformaldehyde for 10 min, permeabilization, and several washing steps, immunofluorescent analyses were performed using polyclonal rabbit anti-human KLF4 (1:100, PA5-27441, Thermo Fisher Scientific), rabbit anti-vascular endothelial (VE)-cadherin (1:100, ab33168, Abcam, Cambridge, United Kingdom), CytoPainter Phalloidin-iFluor 488 (1:1,000, ab176753, Abcam), mouse anti-human KLF2 (1:88, MAB5466, R&D Systems, Minneapolis, Minnesota, United States of America), monoclonal mouse anti-human vWF (1:100, MA5-14029, Thermo Fisher Scientific), Alexa Fluor 488-conjugated secondary goat anti-mouse IgG antibody (A-11029, Thermo Fisher Scientific), Alexa Fluor 555-conjugated goat anti-mouse IgG antibody (ab150114, Abcam) or Alexa Fluor 555-conjugated goat anti-rabbit IgG antibody (A-21429, Thermo Fisher Scientific). DAPI (D9542, Sigma-Aldrich) was used to stain cell nuclei and image acquisition was performed with either an EVOS FL (Thermo Fisher Scientific) or a Zeiss LSM980 Airyscan 2 microscope (Zeiss, Jena, Germany) after addition of mounting medium (50001, Ibidi, Gräfelfing, Germany). After the sensitivity and specificity of VWF staining had been verified, the focus was placed on the *CCM1*^{-/-} cells in direct comparisons to avoid overexposure.

High-Content Imaging

Quantification of WPBs was performed on cells grown on glass bottom imaging plates (Eppendorf, Hamburg, Germany) and following secretagogues treatment using a high-content imaging microscope (Operetta CLS; Perkin Elmer, Waltham, MA, United States). In addition to the digital phase contrast channel (pseudo-cytosolic signal), the images were acquired in three z-planes to detect VWF-positive granula (λ_{ex} 475 nm/ λ_{em} 500–550 nm) and DAPI-stained nuclei (λ_{ex} 365 nm/ λ_{em} 430–500 nm). The algorithm-driven image quantification was performed utilizing the Harmony 4.9 (Perkin Elmer) imaging and analysis software. The images were combined with their maximum projection intensities from all three z-planes and flatfield-adjusted. Per treatment and cell type, at least 2,500 cells in a total of 27 fields of view have been included in the analysis. The nuclei were segmented by their DAPI signal, followed by detection of the surrounding cytosolic area. A selection step was applied to exclude border region objects and dead cells with fragmented nuclei. In order to enhance the contrast, a sliding parabola function was applied, which allowed better discrimination of bright objects. Afterward, the number of WPBs and their intensity was determined inside the cytosolic cell region. To assess the amount of WPBs near the cell nucleus, a 5 μm ring-region was calculated and the granules were quantified inside this region.

Biochemical Analyses

To quantify the secretion of VWF, cell culture supernatants were collected and concentrated (Vacuum concentrator centrifuge, UniEquip, Planegg, Germany). Proteins were analyzed in duplicates using Human VWF-A2 DuoSet ELISA (DY2764-05, R&D Systems) and Ancillary Reagent Kit (DY008, R&D Systems) according to the manufacturer's protocol. Absorbance at 450 and 540 nm was measured on a Paradigm platform (Beckman Coulter, Brea, CA, United States). Values were corrected for 540 nm and normalized to untreated cells.

Immunohistochemistry on Tissue Samples

Immunohistochemistry was performed on FFPE tissue slices as described before (Pagenstecher et al., 2009) using vWF antibody (1:100, M616, Dako (Agilent)) following heat induced antigen retrieval in citrate buffer. Staining intensity in the endothelia of CCMs and vessels in the surrounding brain was evaluated semiquantitatively using five tiers ranging from 0 to ++++.

Statistical Analyses

Data analysis was performed using GraphPad prism software (GraphPad Software, San Diego, CA, United States). Multiple t tests or two-way ANOVA were used for statistical analysis. Where appropriate, Šidák or Dunnet corrections for multiple comparisons were used. For quantification of ELISA data, VWF concentrations were calculated from the standard curve by linear regression performed with the Origin software (Northampton, MA, United States). The standard curve was obtained by fitting the Hill equation [$y = V_{\text{max}} * x^n / (k^n + x^n)$] to our data, with $V_{\text{max}} = 6.00716$, $k = 8,210.36$, $n = 0.72$, and $R^2 = 0.99319$. * $p < 0.05$, ** $p < 0.01$, *** $p < 0.001$, **** $p < 0.0001$.

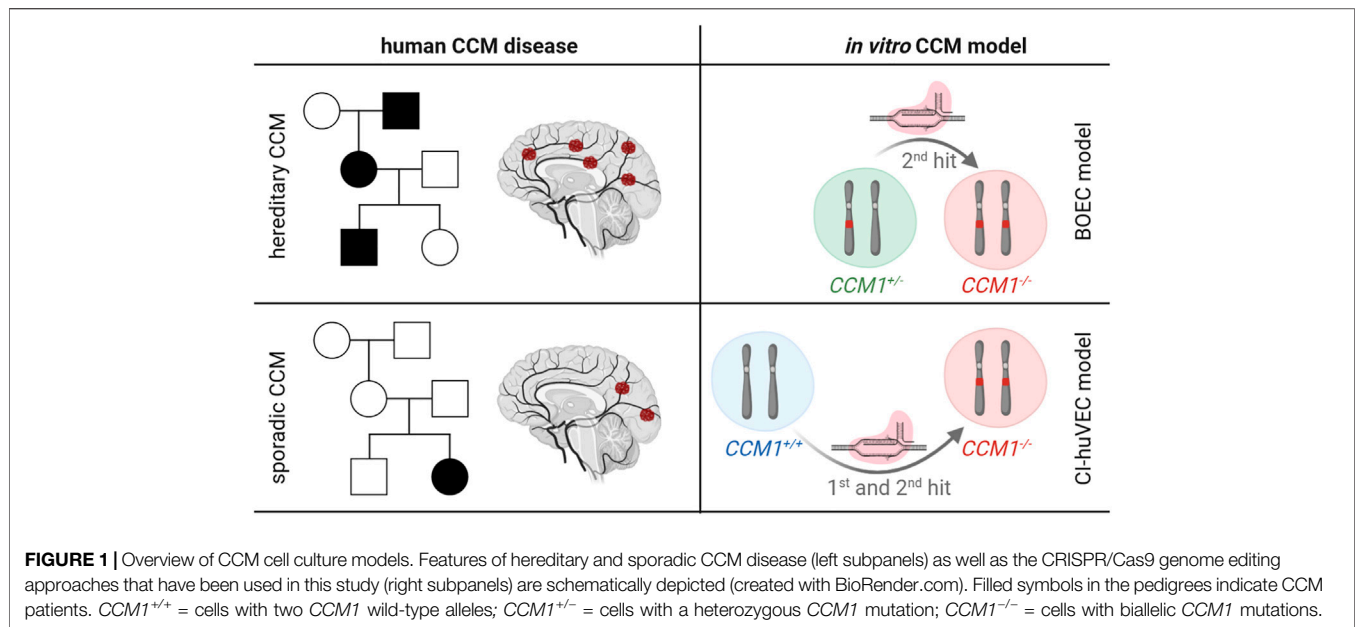
RESULTS

Modeling Hereditary and Sporadic CCM Disease *In Vitro*

To model the hereditary and sporadic type of CCM disease *in vitro* (Figure 1), we used BOECs isolated from peripheral blood of a CCM proband with a heterozygous *CCM1* loss-of-function germline variant (*CCM1*^{+/-}) and wild-type CI-huVECs (*CCM1*^{+/+}). Using CRISPR/Cas9 genome editing, we inactivated the *CCM1* wild-type allele in *CCM1*^{+/-} BOECs or induced biallelic frameshift variants in *CCM1*^{+/+} CI-huVECs and thereby generated pairs of *CCM1*^{+/-} and *CCM1*^{-/-} BOECs (hereditary CCM model) or *CCM1*^{+/+} and *CCM1*^{-/-} CI-huVECs (sporadic CCM model), respectively.

CCM1^{-/-} BOECs Reflect Key Features of CCM Disease

To study the effects of second-hit inactivation of *CCM1* in human ECs, we first established thirty clonal *CCM1*^{-/-} BOEC lines in a single cell cloning approach (Figure 2A). NGS amplicon sequencing verified compound heterozygosity for the pre-existing *CCM1* germline variant and a second CRISPR/Cas9-induced mutation that led to inactivation of the *CCM1* wild-type allele (Figure 2B, Supplementary Table S1). Further cell line



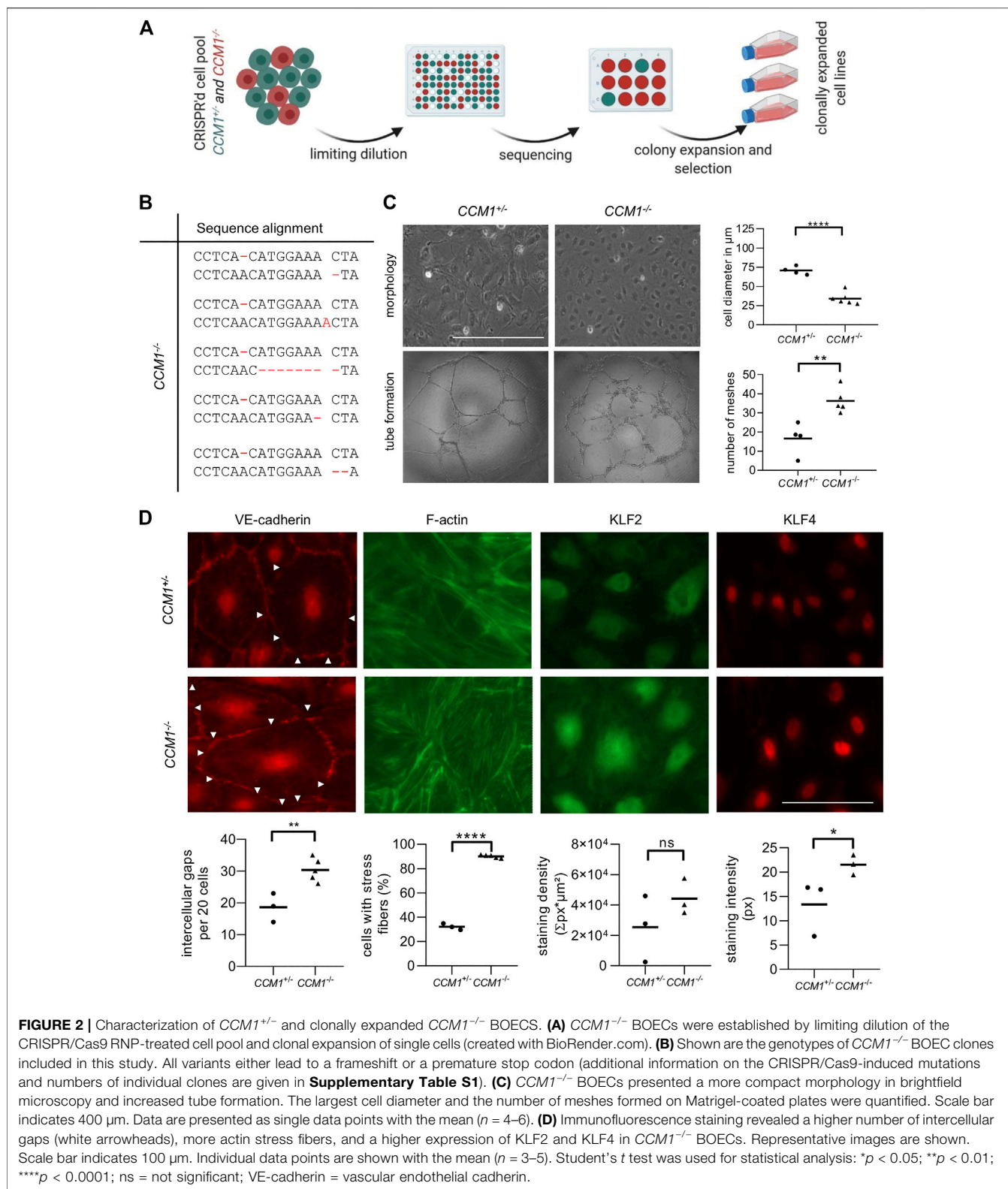
characterizations demonstrated striking differences between $CCM1^{-/-}$ and $CCM1^{+/-}$ BOECs in terms of cell morphology, angiogenic properties, integrity of intercellular junctions, and organization of the actin cytoskeleton. While $CCM1^{+/-}$ BOECs had a cell diameter of 70 μm in two-dimensional monolayer culture, $CCM1^{-/-}$ BOECs presented a more compact morphology with a diameter of only 34.2 μm . In addition, the number of meshes formed by $CCM1^{-/-}$ BOECs on Matrigel-coated plates was significantly increased by 118% (Figure 2C). We also examined the integrity of endothelial adherens junctions as this is a main determinant of vascular permeability (Figure 2D). Remarkably, VE-cadherin staining revealed a 62,6% increase of intercellular gaps upon second-hit inactivation of $CCM1$ in BOECs. While stress fibers (SF) were found in only 32% of $CCM1^{+/-}$ BOECs, over 90% of $CCM1^{-/-}$ BOECs were SF-positive (Figure 2D). The misregulation of actin cytoskeleton dynamics in $CCM1^{-/-}$ BOECs further reinforced that our BOEC model reflects key features of CCM pathophysiology. Since the zinc finger transcription factors KLF2 und KLF4 have been reported as drivers of CCM disease (Renz et al., 2015; Zhou et al., 2016), we decided to address KLF2/4 expression in our *in vitro* model of hereditary CCM disease. KLF4 levels were significantly increased in $CCM1^{-/-}$ BOECs (Figure 2D). Furthermore, a significant upregulation of KLF2 mRNA (Supplementary Figure S1), and a trend towards increased KLF2 expression on protein level were found in $CCM1^{-/-}$ BOECs (Figure 2D).

CCM1 Gene Disruption Induces High-Level VWF Expression and WPB Redistribution in BOECs

Immunofluorescence staining unexpectedly revealed a significant enrichment of the endothelial marker protein VWF in clonally expanded $CCM1^{-/-}$ BOECs when compared to $CCM1^{+/-}$ BOECs

(Figure 3A). Targeted next generation sequencing of all coding exons and exon-intron junctions revealed no VWF variant which might affect gene expression or VWF secretion. Since the endothelium is the main source of plasma VWF (Nichols et al., 2008), we asked the question of whether VWF secretion might be impaired upon complete $CCM1$ inactivation in human ECs. Hence, VWF levels in cell culture supernatants were analyzed by ELISA. Notably, the responsiveness of $CCM1^{-/-}$ BOECs to stimulation with histamine which triggers Ca^{2+} -mediated VWF secretion and the potent non-physiological secretagogue PMA was intact and the secreted VWF levels were not significantly different between $CCM1^{+/-}$ and $CCM1^{-/-}$ BOECs (Figure 3B). To determine alterations of the morphology and intracellular distribution of WPBs upon second-hit inactivation of $CCM1$, their length and the number of WPBs in the perinuclear region were quantified by observer-independent high-content imaging (Figure 3C). WPBs were slightly longer in $CCM1^{-/-}$ BOECs (2.84 μm vs. 2.76 μm under basal conditions, $p = 0.001$; data not shown). Interestingly, a perinuclear accumulation of WPBs was found in unstimulated $CCM1^{+/-}$ BOECs. Stimulation with histamine, PMA or the vasopressin analog DDAVP which triggers cAMP-mediated exocytosis, reduced the number of WPBs in the perinuclear region of $CCM1^{+/-}$ BOECs (Figures 3D,E and Supplementary Figure S2). In unstimulated $CCM1^{-/-}$ BOECs, however, WPBs did not accumulate in the perinuclear region (Figures 3D,E). Additionally, only histamine treatment, but not stimulation with either PMA or DDAVP, induced an additional translocation of WPBs and further reduced their number in the perinuclear region of $CCM1^{-/-}$ BOECs (Figures 3D,E and Supplementary Figure S2).

In conclusion, the CRISPR/Cas9-induced second-hit inactivation of $CCM1$ had caused a VWF reduction in the perinuclear region comparable to the level seen after stimulation with secretagogues in heterozygous $CCM1^{+/-}$ BOECs. These changes most likely reflect a constitutively activated state of $CCM1^{-/-}$ BOECs.



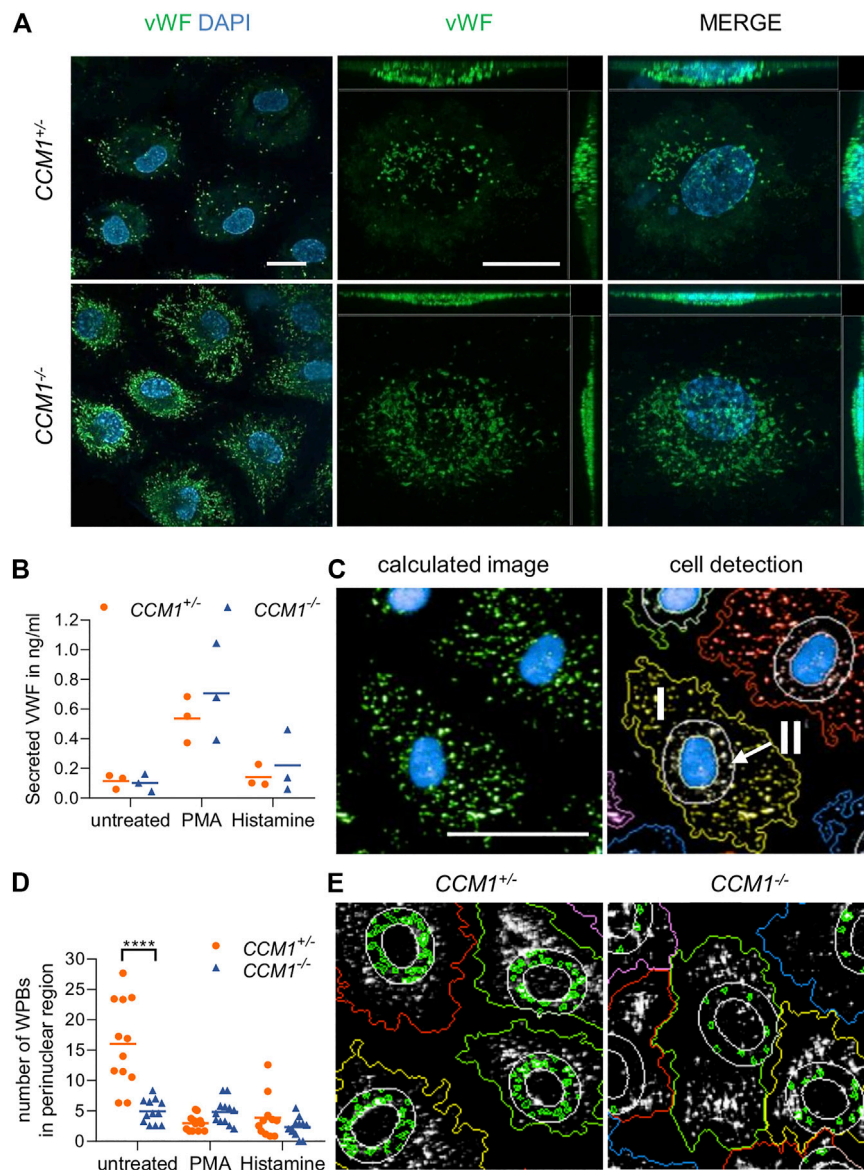
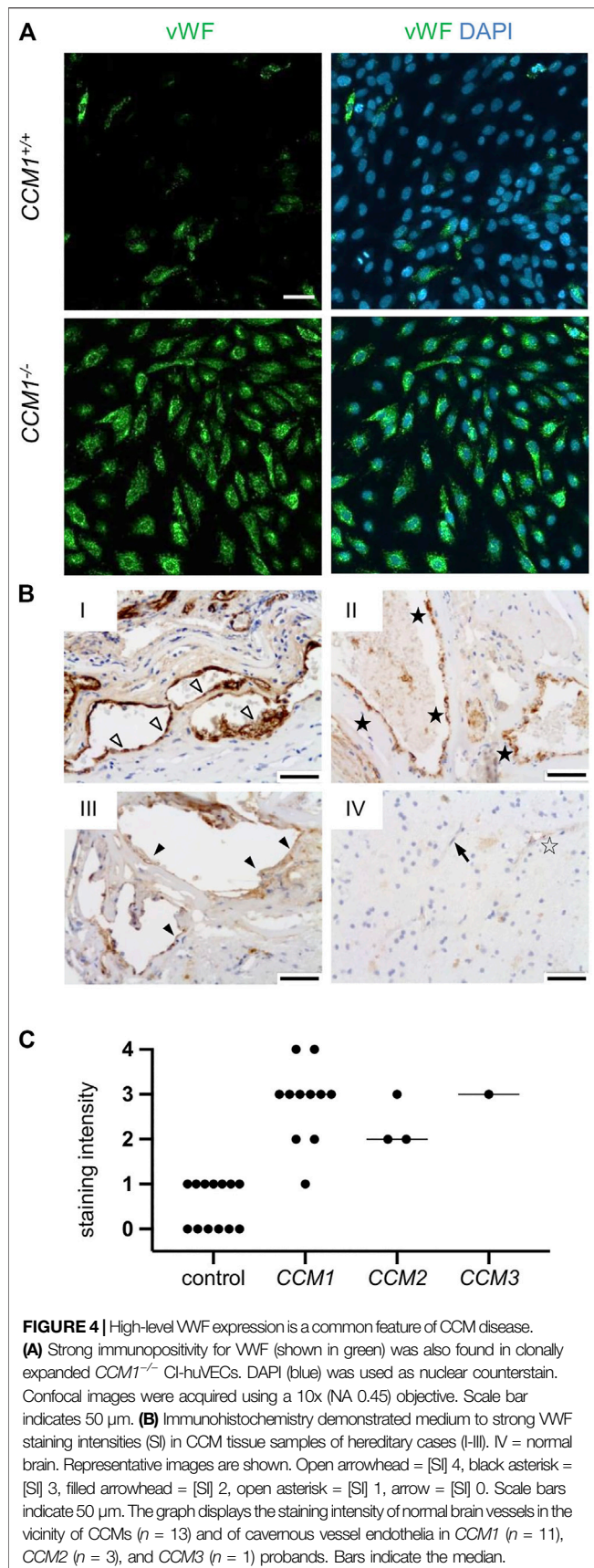


FIGURE 3 | High VWF content and aberrant WPB distribution in *CCM1*^{-/-} BOECs. **(A)** Immunofluorescent staining demonstrated high-level VWF expression (green) in clonally expanded *CCM1*^{-/-} BOECs. DAPI (blue) was used as nuclear counterstain. Confocal images were acquired using a 63x (NA 1.4) oil objective (left) and at higher magnification shown as maximum intensity projection of image stacks (0.2 μm z planes). Scale bars indicate 20 μm. **(B)** Absolute amount of secreted VWF from *CCM1*^{+/-} and *CCM1*^{-/-} BOECs as quantified by ELISA. Data are presented as single data points with the mean (*n* = 3). **(C)** Analysis strategy of high-content imaging for untreated and stimulated BOECs. As basis for quantification, a sliding parabola function was applied for contrast enhancement of the VWF signal (green). Cell nuclei were segmented by their DAPI signal (blue) and the surrounding cytosolic area and perinuclear region were detected. VWF-positive granules in the cytosol (I) and the perinuclear region (II) were quantified. Scale bar indicates 30 μm. **(D)** WPBs in the perinuclear region were quantified as shown in untreated *CCM1*^{+/-} and *CCM1*^{-/-} BOECs. Data are presented as single data points with the mean. Two-way ANOVA with Šidák correction for multiple comparisons was used for statistical analysis. *p* < 0.05. All experiments were performed in triplicates and four biological replicates. **(E)** Representative images of WPBs in the perinuclear region in untreated *CCM1*^{+/-} (left) and *CCM1*^{-/-} BOECs (right).

High VWF Levels in CI-huVECs after CCM1/2/3 Protein Inactivation and in the Endothelium of Human CCMs

VWF levels have recently been reported as marker for the proliferation capacity of individual BOEC clones (de Boer et al., 2020) which are also called endothelial colony forming

cells (Nowak-Sliwinska et al., 2018). Furthermore, changes in VWF expression might also indicate different stages of aging and endothelial-to-mesenchymal transition of BOECs in cell culture (de Jong et al., 2019; de Boer et al., 2020). In a next step, we therefore used immortalized CI-huVECs which represent a well characterized EC culture model (Heiss et al., 2015; Lipps et al., 2018). In line with our observations in *CCM1*^{-/-} BOECs, clonally



expanded $CCM1^{-/-}$ CI-huVECs presented strong immunopositivity for VWF (**Figure 4A**). The same outcome was seen in CI-huVECs that had been treated with $CCM1$ -, $CCM2$ - or $CCM3$ -specific crRNA:tracrRNA:Cas9 RNPs (**Supplementary figure S3**).

Finally, we validated our *in vitro* data in formalin-fixed, paraffin-embedded CCM tissue samples of fifteen probands with a pathogenic germline variant in either $CCM1$, $CCM2$ or $CCM3$ and loss of CCM protein expression in the CCM endothelium (Pagenstecher et al., 2009). In accordance with our *in vitro* data, immunohistochemical analyses demonstrated high VWF signals in endothelial cells lining distended caverns (**Figures 4B,C**).

DISCUSSION

Identifying a molecular explanation for the bleeding tendency of CCMs has been defined as one of the top research priorities by patients and health-care providers (Al-Shahi Salman et al., 2016). Following this recommendation, we here demonstrate the value of CRISPR/Cas9 genome editing in modeling hereditary and sporadic CCM disease *in vitro*, add VWF to the growing list of molecules involved in CCM pathogenesis, and support the hypothesis that a local hemostatic imbalance contributes to thrombosis and hemorrhage in CCMs.

Genome editing has become a powerful tool to model complex human diseases *in vitro*. We have previously used the CRISPR/Cas9 technology for targeted correction of the $CCM1$ mutant allele and second-hit inactivation of $CCM1$ in $CCM1^{+/-}$ BOECs. However, the low clonogenicity of $CCM1^{+/-}$ BOECs and the survival advantage of $CCM1^{-/-}$ BOECs hampered our efforts to fully mimic CCM lesion genesis *in vitro* (Spiegler et al., 2019). Hence, we have now combined our BOEC model which perfectly reproduces the two-hit inactivation mechanism of hereditary CCM ($CCM1^{+/-}$ vs. $CCM1^{-/-}$) with our CI-huVEC model which mimics sporadic CCM disease ($CCM1^{+/+}$ vs. $CCM1^{-/-}$). Well-known features of CCM pathobiology such as actin stress fiber formation, disruption of the integrity of intercellular junctions or upregulation of the transcription factors KLF2 and KLF4 (Glading et al., 2007; Schneider et al., 2011; Faurobert et al., 2013; Shenkar et al., 2015; Cuttano et al., 2016; Zhou et al., 2016) were recapitulated in this cell culture model.

Furthermore, we addressed a new aspect of the hemostatic imbalance in CCMs. CCM bleeding is one of the major concerns of CCM patients and their doctors. Since the risk of future bleeding events is even increased after a first hemorrhage (Al-Shahi Salman et al., 2012), the existence of an anticoagulant micromilieu in CCMs seems plausible (Lopez-Ramirez et al., 2019). However, the frequent observation of thrombi in caverns and nonhemorrhagic focal neurological deficits in CCM patients (Abe et al., 2005; Al-Shahi Salman et al., 2008; Cortes Vela et al., 2012; Horne et al., 2016) suggest a more complex interplay of pro- and anticoagulatory processes in CCM disease. High VWF levels in ECs upon $CCM1$, $CCM2$ or $CCM3$ gene disruption and, most importantly, the striking VWF

immunopositivity within the lining endothelium of individual caverns of human CCMs support this hypothesis. Since stimulation with secretagogues induced proper VWF secretion in *CCM1*^{-/-} BOECs, it is reasonable to assume that vascular stasis and transient procoagulant stimuli trigger local thrombus formation in cavernous lesions. The high affinity of thrombin for the anticoagulant endothelial receptor thrombomodulin which is strongly expressed on ECs of capillaries in the wall of cavernous blood vessels (Abe et al., 2005), may, on the other hand, confer limited protection against thrombosis at the cost of potential bleeding (Lopez-Ramirez et al., 2019). Loose intercellular junctions and recapillarization of organizing thrombi may further promote repeated microhemorrhages into the neighboring brain tissue.

VWF secretion and WPB distribution inside ECs are controlled by a highly regulated molecular network. The secretagogues histamine, DDAVP, and PMA used in this study cover the most important signaling cascades of WPB exocytosis from human ECs (Schillemans et al., 2019). Remarkably, stimulation of *CCM1*^{-/-} BOECs with these secretagogues demonstrated that the second-hit inactivation of *CCM1* does not attenuate the regulated exocytosis of WPBs. Although we cannot exclude that other stimuli such as forskolin, epinephrine, thrombin or VEGF (Rondaj et al., 2006) might have a different effect on *CCM1*-deficient ECs, our observations point to increased intracellular storage of VWF upon *CCM1* inactivation. Besides cAMP- or Ca²⁺-dependent pathways, Rab proteins that are recruited to WPB, the dynein-dynactin complex, the SNARE machinery, the transcription factor KLF2, and various other signaling pathways influence the formation and secretion of WPBs (Rondaj et al., 2006; van Agtmaal et al., 2012; Nightingale and Cutler, 2013; Mourik and Eikenboom, 2017). The observations from our present study suggest that *CCM1* modulates this dynamic process in a KLF2-dependent manner. Upregulation of *KLF2* is a key feature of CCM disease and was also observed in our *in vitro* model. Its misexpression interferes with endothelial quiescence and increases Rho as well as ADAMTS activity (Renz et al., 2015; Zhou et al., 2016). Lentiviral overexpression of *KLF2* in BOECs has been shown to increase the number of WPBs and reduce perinuclear WPB clustering (van Agtmaal et al., 2012). Furthermore, an increase in *VWF* mRNA with a simultaneous decrease in *ANGPT2* mRNA was described in HUVECs upon *KLF2* overexpression (Dekker et al., 2006). These are observations that were also made in our *CCM1*^{-/-} BOEC model. Despite upregulation of *KLF2* in *CCM1*^{-/-} BOEC, we did not observe a shortening of WPBs which would have been indicative of reduced activity of primary hemostasis (Ferraro et al., 2016; Ferraro et al., 2020). In fact, we even found slightly longer WPBs in *CCM1*-depleted ECs. An increased fraction of longer WPBs can be associated with a higher prothrombotic potential because they contain substantial VWF amounts (Ferraro et al., 2014; Ferraro et al., 2016). It is probably selective exocytosis of these long WPB that might be affected by *CCM1* depletion. The group of Daniel Cutler recently demonstrated that the release of large WPBs requires the recruitment of an actin ring while the exocytosis of smaller WPBs does not (McCormack et al., 2020). Interestingly,

reorganization of the actin cytoskeleton, particularly the decrease of cortical actin filaments and the increased formation of actin stress fibers, is one of the most studied effects of CCM protein depletion in human ECs (Figure 2D); (Glading et al., 2007; Faurobert et al., 2013; Schwefel et al., 2019; Spiegler et al., 2019; Schwefel et al., 2020). Specific actin-dependent exocytosis alterations might also be an explanation why the secretion of other WPB components can be normal or even increased in *CCM1*-, *CCM2*- or *CCM3*-depleted ECs as these smaller molecules can also be released by kiss-and-run or actin-independent full fusion.

In conclusion, our results point to the co-existence of pro- and anticoagulatory processes in CCM which provides an explanation for the favorable outcome seen in CCM patients who got antithrombotic therapies for other reasons (Schneble et al., 2012; Zuurbier et al., 2019). Future randomized trials will have to show whether therapies addressing hemostasiological homeostasis are not only safe for CCM patients but also have a therapeutic effect on the bleeding tendency of their CCMs.

DATA AVAILABILITY STATEMENT

The original contributions presented in the study are included in the article/**Supplementary Material**, further inquiries can be directed to the corresponding author.

ETHICS STATEMENT

The studies involving human participants were reviewed and approved by the local ethics committee of the University Medicine Greifswald, Germany (No: BB 047/14a). The patients/participants provided their written informed consent to participate in this study.

AUTHOR CONTRIBUTIONS

CDM, BSS, KS, and SS performed the experiments. CDM, MR, UF, and SS contributed to the intellectual conception and the design of the study. MR, UF, and SS supervised the experiments. CDM, BSS, MR, OO, and SS analyzed the data. EF and SB executed the high-throughput imaging analysis. AP performed the immunohistochemistry of tissue samples. All authors supported in data interpretation. MR, UF, and SS drafted the manuscript and all authors participated in writing.

FUNDING

This work was funded by grants from the Research Network Molecular Medicine of the University Medicine Greifswald to SS (FVMM, Grant No FOVB-2017-03, FOVB-2018-06). MR was supported by the German Research Foundation (DFG RA2876/2-2). SB received a grant from the German Federal Ministry of Education and Research (BMBF, 03Z22DN11).

ACKNOWLEDGMENTS

Andreas Greinacher is thanked for fruitful discussions and comments on the manuscript. Doreen Biedenweg and Heike Geißel are thanked for excellent technical assistance.

REFERENCES

- Abe, M., Fukudome, K., Sugita, Y., Oishi, T., Tabuchi, K., and Kawano, T. (2005). Thrombus and Encapsulated Hematoma in Cerebral Cavernous Malformations. *Acta Neuropathol.* 109 (5), 503–509. doi:10.1007/s00401-005-0994-8
- Akers, A. L., Johnson, E., Steinberg, G. K., Zabramski, J. M., and Marchuk, D. A. (2009). Biallelic Somatic and Germline Mutations in Cerebral Cavernous Malformations (CCMs): Evidence for a Two-Hit Mechanism of CCM Pathogenesis. *Hum. Mol. Genet.* 18 (5), 919–930. doi:10.1093/hmg/ddn430
- Akers, A., Al-Shahi Salman, R., A. Awad, I., Dahlem, K., Flemming, K., Hart, B., et al. (2017). Synopsis of Guidelines for the Clinical Management of Cerebral Cavernous Malformations: Consensus Recommendations Based on Systematic Literature Review by the Angioma Alliance Scientific Advisory Board Clinical Experts Panel. *Neurosurgery* 80 (5), 665–680. doi:10.1093/neuros/nyx091
- Al-Shahi Salman, R., Berg, M. J., Morrison, L., Awad, I. A., and Angioma Alliance Scientific Advisory, B. (2008). Hemorrhage from Cavernous Malformations of the Brain: Definition and Reporting Standards. Angioma Alliance Scientific Advisory Board. *Stroke* 39 (12), 3222–3230. doi:10.1161/STROKEAHA.108.515544
- Al-Shahi Salman, R., Hall, J. M., Horne, M. A., Moultrie, F., Josephson, C. B., Bhattacharya, J. J., et al. (2012). Scottish Audit of Intracranial Vascular Malformations C (2012). Untreated Clinical Course of Cerebral Cavernous Malformations: a Prospective, Population-Based Cohort Study. *Lancet Neurol.* 11 (3), 217–224. doi:10.1016/S1474-4422(12)70004-2
- Al-Shahi Salman, R., Kitchen, N., Thomson, J., Ganesan, V., Mallucci, C., and Radatz, M. (2016). Cavernoma Priority Setting Partnership Steering G (2016). Top Ten Research Priorities for Brain and Spine Cavernous Malformations. *Lancet Neurol.* 15 (4), 354–355. doi:10.1016/S1474-4422(16)00039-9
- Cortés Vela, J. J., Concepción Aramendía, L., Ballenilla Marco, F., Gallego León, J. I., and González-Spínola San Gil, J. (2012). Cerebral Cavernous Malformations: Spectrum of Neuroradiological Findings. *Radiologia (English Edition)* 54 (5), 401–409. doi:10.1016/j.rx.2011.09.016.1016/j.rxeng.2011.09.004
- Cuttano, R., Rudini, N., Bravi, L., Corada, M., Giampietro, C., Papa, E., et al. (2016). KLF4 Is a Key Determinant in the Development and Progression of Cerebral Cavernous Malformations. *EMBO Mol. Med.* 8 (1), 6–24. doi:10.15252/emmm.201505433
- Boer, S., Bowman, M., Notley, C., Mo, A., Lima, P., Jong, A., et al. (2020). Endothelial Characteristics in Healthy Endothelial Colony Forming Cells: Generating a Robust and Valid *Ex Vivo* Model for Vascular Disease. *J. Thromb. Haemost.* 18, 2721–2731. doi:10.1111/jth.14998
- Jong, A., Weijers, E., Dirven, R., Boer, S., Streur, J., and Eikenboom, J. (2019). Variability of Von Willebrand Factor-Related Parameters in Endothelial Colony Forming Cells. *J. Thromb. Haemost.* 17 (9), 1544–1554. doi:10.1111/jth.14558
- Dekker, R. J., Boon, R. A., Rondaij, M. G., Kragt, A., Volger, O. L., Elderkamp, Y. W., et al. (2006). KLF2 Provokes a Gene Expression Pattern that Establishes Functional Quiescent Differentiation of the Endothelium. *Blood* 107 (11), 4354–4363. doi:10.1182/blood-2005-08-3465
- Detter, M. R., Snellings, D. A., and Marchuk, D. A. (2018). Cerebral Cavernous Malformations Develop through Clonal Expansion of Mutant Endothelial Cells. *Circ. Res.* 123 (10), 1143–1151. doi:10.1161/CIRCRESAHA.118.313970
- Erent, M., Meli, A., Moiso, N., Babich, V., Hannah, M. J., Skehel, P., et al. (2007). Rate, Extent and Concentration Dependence of Histamine-Evoked Weibel-Palade Body Exocytosis Determined from Individual Fusion Events in Human Endothelial Cells. *J. Physiol.* 583 (Pt 1), 195–212. doi:10.1113/jphysiol.2007.132993

SUPPLEMENTARY MATERIAL

The Supplementary Material for this article can be found online at: <https://www.frontiersin.org/articles/10.3389/fmolb.2021.622547/full#supplementary-material>

- Faurobert, E., Rome, C., Lisowska, J., Manet-Dupé, S., Boulday, G., Malbouyres, M., et al. (2013). CCM1-ICAP-1 Complex Controls β 1 Integrin-dependent Endothelial Contractility and Fibronectin Remodeling. *J. Cel. Biol.* 202 (3), 545–561. doi:10.1083/jcb.201303044
- Ferraro, F., Kriston-Vizi, J., Metcalf, D. J., Martin-Martin, B., Freeman, J., Burden, J. J., et al. (2014). A Two-Tier Golgi-Based Control of Organelle Size Underpins the Functional Plasticity of Endothelial Cells. *Dev. Cel.* 29 (3), 292–304. doi:10.1016/j.devcel.2014.03.021
- Ferraro, F., da Silva, M. L., Grimes, W., Lee, H. K., Ketteler, R., Kriston-Vizi, J., et al. (2016). Weibel-Palade Body Size Modulates the Adhesive Activity of its von Willebrand Factor Cargo in Cultured Endothelial Cells. *Sci. Rep.* 6, 32473. doi:10.1038/srep32473
- Ferraro, F., Patella, F., Costa, J. R., Ketteler, R., Kriston-Vizi, J., and Cutler, D. F. (2020). Modulation of Endothelial Organelle Size as an Antithrombotic Strategy. *J. Thromb. Haemost.* 18 (12), 3296–3308. doi:10.1111/jth.15084
- Flemming, K. D., and Lanzino, G. (2020). Cerebral Cavernous Malformation: What a Practicing Clinician Should Know. *Mayo Clinic Proc.* 95, 2005–2020. doi:10.1016/j.mayocp.2019.11.005
- Gault, J., Shenkar, R., Recksiek, P., and Awad, I. A. (2005). Biallelic Somatic and Germ Line CCM1 Truncating Mutations in a Cerebral Cavernous Malformation Lesion. *Stroke* 36 (4), 872–874. doi:10.1161/01.STR.0000157586.20479.f4
- Glading, A., Han, J., Stockton, R. A., and Ginsberg, M. H. (2007). KRIT-1/CCM1 Is a Rap1 Effector that Regulates Endothelial Cell-Cell Junctions. *J. Cel. Biol.* 179 (2), 247–254. doi:10.1083/jcb.200705175
- Heiss, M., Hellström, M., Kalén, M., May, T., Weber, H., Hecker, M., et al. (2015). Endothelial Cell Spheroids as a Versatile Tool to Study Angiogenesis *In Vitro*. *FASEB j.* 29 (7), 3076–3084. doi:10.1096/fj.14-267633
- Hong, C. C., Tang, A. T., Detter, M. R., Choi, J. P., Wang, R., Yang, X., et al. (2020). Cerebral Cavernous Malformations Are Driven by ADAMTS5 Proteolysis of Versican. *J. Exp. Med.* 217 (10), e20200140. doi:10.1084/jem.20200140
- Horne, M. A., Flemming, K. D., Su, I.-C., Stapf, C., Jeon, J. P., Li, D., et al. (2016). Clinical Course of Untreated Cerebral Cavernous Malformations: a Meta-Analysis of Individual Patient Data. *Lancet Neurol.* 15 (2), 166–173. doi:10.1016/S1474-4422(15)00303-8
- Laberge-le Couteux, S., Jung, H. H., Labauge, P., Houtteville, J.-P., Lescoat, C., Cecillon, M., et al. (1999). Truncating Mutations in CCM1, Encoding KRIT1, Cause Hereditary Cavernous Angiomas. *Nat. Genet.* 23 (2), 189–193. doi:10.1038/13815
- Lip, G., and Blann, A. (1997). Von Willebrand Factor: a Marker of Endothelial Dysfunction in Vascular Disorders? *Cardiovasc. Res.* 34 (2), 255–265. doi:10.1016/s0008-6363(97)00039-4
- Lipps, C., Klein, F., Wahlich, T., Seiffert, V., Butueva, M., Zauers, J., et al. (2018). Expansion of Functional Personalized Cells with Specific Transgene Combinations. *Nat. Commun.* 9 (1), 994. doi:10.1038/s41467-018-03408-4
- Loesberg, C., Gonsalves, M. D., Zandbergen, J., Willems, C., van Aken, W. G., Stel, H. V., et al. (1983). The Effect of Calcium on the Secretion of Factor VIII-Related Antigen by Cultured Human Endothelial Cells. *Biochim. Biophys. Acta (Bba) - Mol. Cel. Res.* 763 (2), 160–168. doi:10.1016/0167-4889(83)90039-3
- Lopez-Ramirez, M. A., Pham, A., Girard, R., Wyseure, T., Hale, P., Yamashita, A., et al. (2019). Cerebral Cavernous Malformations Form an Anticoagulant Vascular Domain in Humans and Mice. *Blood* 133 (3), 193–204. doi:10.1182/blood-2018-06-856062
- Maddaluno, L., Rudini, N., Cuttano, R., Bravi, L., Giampietro, C., Corada, M., et al. (2013). EndMT Contributes to the Onset and Progression of Cerebral Cavernous Malformations. *Nature* 498 (7455), 492–496. doi:10.1038/nature12207
- Malinverno, M., Maderna, C., Abu Taha, A., Corada, M., Orsenigo, F., Valentino, M., et al. (2019). Endothelial Cell Clonal Expansion in the Development of Cerebral Cavernous Malformations. *Nat. Commun.* 10 (1), 2761. doi:10.1038/s41467-019-10707-x

- McCormack, J. J., Harrison-Lavoie, K. J., and Cutler, D. F. (2020). Human Endothelial Cells Size-select Their Secretory Granules for Exocytosis to Modulate Their Functional Output. *J. Thromb. Haemost.* 18 (1), 243–254. doi:10.1111/jth.14634
- McDonald, D. A., Shi, C., Shenkar, R., Gallione, C. J., Akers, A. L., Li, S., et al. (2014). Lesions from Patients with Sporadic Cerebral Cavous Malformations Harbor Somatic Mutations in the CCM Genes: Evidence for a Common Biochemical Pathway for CCM Pathogenesis. *Hum. Mol. Genet.* 23 (16), 4357–4370. doi:10.1093/hmg/ddu153
- Mourik, M., and Eikenboom, J. (2017). Lifecycle of Weibel-Palade Bodies. *Hamostaseologie* 37 (1), 13–24. doi:10.5482/HAMO-16-07-0021
- Nichols, W. L., Hultin, M. B., James, A. H., Manco-Johnson, M. J., Montgomery, R. R., Ortel, T. L., et al. (2008). Von Willebrand Disease (VWD): Evidence-Based Diagnosis and Management Guidelines, the National Heart, Lung, and Blood Institute (NHLBI) Expert Panel Report (USA). *Haemophilia* 14 (2), 171–232. doi:10.1111/j.1365-2516.2007.01643.x
- Nightingale, T., and Cutler, D. (2013). The Secretion of von Willebrand Factor from Endothelial Cells; an Increasingly Complicated Story. *J. Thromb. Haemost.* 11 Suppl. 1 (Suppl 1), 192–201. doi:10.1111/jth.12225
- Nowak-Sliwinska, P., Alitalo, K., Allen, E., Anisimov, A., Aplin, A. C., Auerbach, R., et al. (2018). Consensus Guidelines for the Use and Interpretation of Angiogenesis Assays. *Angiogenesis* 21 (3), 425–532. doi:10.1007/s10456-018-9613-x
- Pagenstecher, A., Stahl, S., Sure, U., and Felbor, U. (2009). A Two-Hit Mechanism Causes Cerebral Cavous Malformations: Complete Inactivation of CCM1, CCM2 or CCM3 in Affected Endothelial Cells. *Hum. Mol. Genet.* 18 (5), 911–918. doi:10.1093/hmg/ddn420
- Rath, M., Pagenstecher, A., Hoischen, A., and Felbor, U. (2020). Postzygotic Mosaicism in Cerebral Cavous Malformation. *J. Med. Genet.* 57 (3), 212–216. doi:10.1136/jmedgenet-2019-106182
- Ren, A. A., Snellings, D. A., Su, Y. S., Hong, C. C., Castro, M., Tang, A. T., et al. (2021). *PIK3CA* and CCM Mutations Fuel Cavomas through a Cancer-like Mechanism. *Nature* 594, 271–276. doi:10.1038/s41586-021-03562-8
- Renz, M., Otten, C., Faurobert, E., Rudolph, F., Zhu, Y., Boulday, G., et al. (2015). Regulation of $\beta 1$ Integrin-Klf2-Mediated Angiogenesis by CCM Proteins. *Dev. Cel.* 32 (2), 181–190. doi:10.1016/j.devcel.2014.12.016
- Rondaj, M. G., Bierings, R., Kragt, A., Gijzen, K. A., Sellink, E., van Mourik, J. A., et al. (2006). Dynein-dynactin Complex Mediates Protein Kinase A-dependent Clustering of Weibel-Palade Bodies in Endothelial Cells. *Atvb* 26 (1), 49–55. doi:10.1161/01.ATV.0000191639.08082.04
- Sadler, J. E. (1998). Biochemistry and Genetics of Von Willebrand Factor. *Annu. Rev. Biochem.* 67, 395–424. doi:10.1146/annurev.biochem.67.1.395
- Sahoo, T., Johnson, E. W., Thomas, J. W., Kuehl, P. M., Jones, T. L., Dokken, C. G., et al. (1999). Mutations in the Gene Encoding KRIT1, a Krev-1/rap1a Binding Protein, Cause Cerebral Cavous Malformations (CCM1). *Hum. Mol. Genet.* 8 (12), 2325–2333. doi:10.1093/hmg/8.12.2325
- Schillemans, M., Karampini, E., Kat, M., and Bierings, R. (2019). Exocytosis of Weibel-Palade Bodies: How to Unpack a Vascular Emergency Kit. *J. Thromb. Haemost.* 17 (1), 6–18. doi:10.1111/jth.14322
- Schneble, H.-M., Soumare, A., Hervé, D., Bresson, D., Guichard, J.-P., Riant, F., et al. (2012). Antithrombotic Therapy and Bleeding Risk in a Prospective Cohort Study of Patients with Cerebral Cavous Malformations. *Stroke* 43 (12), 3196–3199. doi:10.1161/STROKEAHA.112.668533
- Schneider, H., Errede, M., Ulrich, N. H., Virgintino, D., Frei, K., and Bertalanffy, H. (2011). Impairment of Tight Junctions and Glucose Transport in Endothelial Cells of Human Cerebral Cavous Malformations. *J. Neuropathol. Exp. Neurol.* 70 (6), 417–429. doi:10.1097/NEN.0b013e31821bc40e
- Schwefel, K., Spiegler, S., Ameling, S., Much, C. D., Pilz, R. A., Otto, O., et al. (2019). Biallelic CCM3 Mutations Cause a Clonogenic Survival Advantage and Endothelial Cell Stiffening. *J. Cel. Mol. Med.* 23 (3), 1771–1783. doi:10.1111/jcmm.14075
- Schwefel, K., Spiegler, S., Kirchmaier, B. C., Dellweg, P. K. E., Much, C. D., Pané-Farré, J., et al. (2020). Fibronectin Rescues Aberrant Phenotype of Endothelial Cells Lacking Either CCM1, CCM2 or CCM3. *FASEB j.* 34, 9018–9033. doi:10.1096/fj.201902888R
- Shenkar, R., Shi, C., Rebeiz, T., Stockton, R. A., McDonald, D. A., Mikati, A. G., et al. (2015). Exceptional Aggressiveness of Cerebral Cavous Malformation Disease Associated with *PDCD10* Mutations. *Genet. Med.* 17 (3), 188–196. doi:10.1038/gim.2014.97
- Spiegler, S., Rath, M., Much, C. D., Sendtner, B. S., and Felbor, U. (2019). Precise CCM1 Gene Correction and Inactivation in Patient-derived Endothelial Cells: Modeling Knudson's Two-hit Hypothesis *In Vitro*. *Mol. Genet. Genomic Med.* 7 (7), e00755. doi:10.1002/mgg3.755
- van Aagtmaal, E. L., Bierings, R., Dragt, B. S., Leyen, T. A., Fernandez-Borja, M., Horrevoets, A. J. G., et al. (2012). The Shear Stress-Induced Transcription Factor KLF2 Affects Dynamics and Angiopoietin-2 Content of Weibel-Palade Bodies. *PLoS One* 7 (6), e38399. doi:10.1371/journal.pone.0038399
- Wagner, D. D., and Frenette, P. S. (2008). The Vessel wall and its Interactions. *Blood* 111 (11), 5271–5281. doi:10.1182/blood-2008-01-078204
- Wang, J.-W., Bouwens, E. A. M., Pintao, M. C., Voorberg, J., Safdar, H., Valentijn, K. M., et al. (2013). Analysis of the Storage and Secretion of Von Willebrand Factor in Blood outgrowth Endothelial Cells Derived from Patients With von Willebrand Disease. *Blood* 121 (14), 2762–2772. doi:10.1182/blood-2012-06-434373
- Weibel, E. R., and Palade, G. E. (1964). New Cytoplasmic Components in Arterial Endothelia. *J. Cel. Biol.* 23, 101–112. doi:10.1083/jcb.23.1.101
- Zhou, Z., Tang, A. T., Wong, W.-Y., Bamezai, S., Goddard, L. M., Shenkar, R., et al. (2016). Cerebral Cavous Malformations Arise from Endothelial Gain of MEKK3-Klf2/4 Signalling. *Nature* 532 (7597), 122–126. doi:10.1038/nature17178
- Zuurbier, S. M., Hickman, C. R., Tolia, C. S., Rinkel, L. A., Leyrer, R., Flemming, K. D., et al. (2019). Scottish Audit of Intracranial Vascular Malformations Steering C (2019). Long-Term Antithrombotic Therapy and Risk of Intracranial Haemorrhage from Cerebral Cavous Malformations: a Population-Based Cohort Study, Systematic Review, and Meta-Analysis. *Lancet Neurol.* 18 (10), 935–941. doi:10.1016/S1474-4422(19)30231-5

Conflict of Interest: The authors declare that the research was conducted in the absence of any commercial or financial relationships that could be construed as a potential conflict of interest.

Copyright © 2021 Much, Sendtner, Schwefel, Freund, Bekeschus, Otto, Pagenstecher, Felbor, Rath and Spiegler. This is an open-access article distributed under the terms of the Creative Commons Attribution License (CC BY). The use, distribution or reproduction in other forums is permitted, provided the original author(s) and the copyright owner(s) are credited and that the original publication in this journal is cited, in accordance with accepted academic practice. No use, distribution or reproduction is permitted which does not comply with these terms.